

Received October 2, 2017, accepted November 2, 2017, date of publication November 28, 2017, date of current version February 14, 2018.

Digital Object Identifier 10.1109/ACCESS.2017.2778004

# Battery Storage for the Utility-Scale Distributed Photovoltaic Generations

NURSYARIZAL MOHD NOR, ABID ALI<sup>✉</sup>, TAIB IBRAHIM, AND MOHD FAKHIZAN ROMLIE

Department of Electrical and Electronic Engineering, Universiti Teknologi PETRONAS, Seri Iskandar 32610, Malaysia

Corresponding author: Abid Ali (powereng1982@gmail.com)

**ABSTRACT** Batteries are essential for efficiently utilizing the energy from the photovoltaic (PV) modules. However, integration of batteries with PV plants at large scale needs more attention in terms of size, location, and times for the charging and discharging of the batteries. This paper addresses these aspects. It presents a mixed integer optimization using genetic algorithm for determining the optimum size and placement of battery-sourced distributed PV generation (B-SDPVG) in distribution networks. The total energy loss index is formulated as the main objective function and simultaneously, the bus voltage deviations and penetrations of the B-SDPVG are calculated. The yields from the PV plants are estimated using 15 years of weather data modeled with the aid of beta probability density function. Furthermore, a novel charge–discharge control model is developed for determining the choice of the charging and discharging of batteries at each hour. By considering different time varying voltage-dependent load models, the proposed algorithm is applied on the IEEE 33 bus and the IEEE 69 bus test distribution networks. The numerical results of two distribution networks with time-varying loads show the advantages of the proposed methodology. It was revealed that integration of battery storage and intelligent scheduling for charging and discharging of batteries produced much better results and improved the quality of distribution networks. The supply of power from the B-SDPVG during the peak load hours and at night was made possible for each load model. The proposed charge–discharge control model for scheduling the charging and discharging of the batteries was found dynamic. Results of this paper can be of potential importance in planning for the integration of battery storage in distribution networks.

**INDEX TERMS** Distributed generation, solar photovoltaic, beta probability density function, radial distribution network, power loss index, genetic algorithm, battery storage, load flow analysis.

## NOMENCLATURE

Beta (s)	Beta distribution function of s
DG	Distributed generation
B-SDPVG	Battery-sourced distributed photovoltaic generation
$E_{\text{loss\_total}}^{\text{B-SDPVG}}$	Annual energy losses with B-SDPVG
GA	Genetic algorithm
GWp	Gigawatt peak
K <sub>i</sub>	Current temperature coefficient A/°C
K <sub>v</sub>	Voltage temperature coefficient V/°C
MIOGA	Mixed Integer Optimization using Genetic Algorithm
NOCT	Nominal temperature of the module 0C
O&M	Operation and maintenance
OPF	Optimal power flow
P(i)	Active power that flow across the branch i.

P(k + 1), eff	Effective active power which is flowing towards bus k + 1 from the other buses
pdf	Probability density function
P <sub>B-SDPVG</sub> (t)	Active power output from B-SDPVG at time t
pf	Power factor
P <sub>loss</sub> (i)	Active power losses across the branch i
P <sub>loss\_total</sub>	Total power losses in whole network
P <sub>Substation</sub> (t)	Active power supplied through the substation at time t
Q(i)	Reactive power that flow across the branch i.
Q <sub>loss</sub> (i)	Active power losses across the branch i
Q <sub>loss\_total</sub>	Total power losses in whole network
Q <sub>(k+1),eff</sub>	Effective reactive power which is flowing towards bus k + 1 from the other buses

$Q_{\text{Substation}}(t)$	Reactive power supplied through the substation at time $t$
RDS	Radial distribution system
$R_i$	Resistance of the branch $i$ ,
$s$	Solar irradiance in $\text{KW/m}^2$
$T_a$	Ambient temperature $^{\circ}\text{C}$
$T_c$	Cell temperature $^{\circ}\text{C}$
TELI	Total energy loss index
$V(k)$	Voltage magnitude of $k$ th bus
$V_{\text{Dev}_{\text{max}}}$	Maximum voltage deviation
$v_r$	Voltage Coefficients For Reactive Loads
$v_{\alpha}$	Voltage coefficients for active loads
$X_i$	Reactance of the branch $i$ ,
$\alpha, \beta$	alpha and beta parameters of Beta pdf
$\eta$	Inverter efficiency
$\mu$	Mean
$\sigma$	Standard deviation

## I. INTRODUCTION

The limitations of reserves and environmental concerns associated with the fossil-fuels have intimidated the development of new power plants that deploy the renewable energy as a source of producing electricity. In recent years, anticipation for the use of power from the sustainable power sources has been extended due to their cost-effectiveness and the ecological points of interest. Among the various renewable energy sources, photovoltaic (PV) technology is receiving more attention due to the increases in efficiency and decreases in the cost of the PV modules [1]. Moreover, the availability of good solar irradiance levels in many countries and ease of operation & maintenance (O&M) of the PV modules are making this technology more favorable [2], [3]. The global PV market has experienced a significant progress in the recent years and with 50 % growth in the year 2016 alone, the worldwide cumulative PV installed capacity is estimated to be more than 300 GWp [4]. Furthermore, it is expected that this figure will exceed 500 GWp by the year 2019 [5]. On one hand, this signifies the generation of carbon-free and low cost electricity in the coming years. On the other hand, it also depicts the utilization of large scale electricity from an intermittent source.

In order to cope with the intermittency of the power outputs, battery storage is considered beneficial to be used with the photovoltaic (PV) systems [6], [7]. Battery storage can be used for storing the energy during the periods when the outputs from the PV modules exceeds the energy demands [8]. Due to high energy density and long cycle life, Lithium-ion batteries (LiBs) are widely studied and used as a source of electric power [9]. LiBs have been used by different applications for many years in the past, and these have started gaining more importance in connection to renewable energy sources in electricity markets in the recent years. In addition to supply of bulk electricity, LiBs are considered suitable for many power system applications, such as increasing the penetration of intermittent sources, enhancement of network reliability (by increasing transmission line capacities),

improving power quality (by alleviating voltage oscillations) and providing power for electric vehicles [10]–[14]. Apart from Lithium-ion batteries (LiBs), supercapacitors (SCs) or ultracapacitors (UCs) are gaining increasing popularity and attention due to their high power density and exceptional durability [15], [16]. However, LiBs are considered suitable due to their lower purchase cost and stable voltage under discharge [17]. With the increasing advancement in renewable energy technology, it is predicted that future electricity infrastructure will include the storage systems together with PV for supplying dispatchable electricity. Several indicators suggest that the cost of electricity produced by a PV-Battery system together, could be much competitive to the cost of electricity produced through PV alone [18]. It is expected that in addition to the reduction of cost of PV modules, the cost of batteries will also reduce in the coming years.

Although there is extensive research on the utilization of energy from the renewable sources [19]–[26], the utilization of battery storage for the distribution networks is not so well researched. Without having any storage source, the outputs from the intermittent DGs are assumed dispatchable. The methodologies in various research studies for sizing of energy storage for large PV plants follow the same techniques, which have been used for standalone PV and hybrid energy systems [27]–[32].

Several recent studies have been reported regarding the potential of including battery storage for enhancing the bus voltage profiles, reducing network loss, efficient utilization of the energy and improving the penetration of intermittent DG. The study for the optimal planning of the battery energy storage systems (BESS) to provide the technical and economic benefits in active distribution system was proposed in [33] and [34]. Furthermore, certain studies have demonstrated the utilization of battery storage for providing power quality benefits [35], [36], minimizing the total net present value (NPV) [37], [38] and reducing the energy losses [39] in electrical distribution networks. Moreover, a cost-based multi-objective optimization strategy using the cost of the system and the cost of battery cycling was presented in [40]. Few studies have investigated battery storage for microgrids [41], [42] and battery storage in distribution networks, considering time-of-use (TOU) prices [43].

The available literature suggests that sizing and placement of battery storage with PV plants at distribution level has been done in viewpoint of economy; whereas, the decision of charging and discharging of batteries depended on the price of electricity purchased by the distribution system. The research methodology in many studies did not include the dynamics for the sizing and utilization mechanism for the energy from the PV/batteries. Batteries are used to fulfill the daily energy demand without knowing the hourly optimum energy levels for discharging of batteries. Batteries are considered to charge during the periods when the power outputs from the DGs were excessive. Whereas, in real time scenarios, the battery charging and discharging operations should consider

the availability and needs of energy from the PV plants and grids.

Moreover, the prices of electricity based on the time-of-use model have not been introduced in many countries. The distribution networks are capable of accepting a fraction of the peak supply rather than peak. For example, for a 3.7 MW load in the IEEE 33 test distribution network, only 2.59 MW is supplied rather than 3.7 MW [19]. In that case, charging of batteries only when the output of the DGs is greater than 3.7 MW would not be recommended. In addition to inaccurate sizing of the batteries, such method would also result in more power losses. Moreover, time and rate of the discharging of batteries has been done without any knowledge of the exact technical benefits to the distribution networks.

The loopholes in the existing methods regarding sizing and utilization of energy from battery storage point towards the need for developing new methods that should address the sizing of PV plants, sizing of battery storage and the scheduling of the battery charging/discharging efficiently.

This paper presents a novel method for the sizing and the utilization of the energy from the Battery-Sourced Distributed Photovoltaic Generation (B-SDPVG) in the distribution networks. A control model is developed, which helps to use the energy from the PV plant and the battery storage more efficiently. The time and the amount of charging and discharging of the batteries are chosen to reduce the total amount of energy losses. The minimization of the total energy losses was considered to be the main objective function; however, the study also monitored the impact of B-SDPVG power on the PV penetration levels and on the deviations in the voltage of the weakest bus in the distribution networks. The study adopted the Mixed Integer Optimization using Genetic Algorithm (MIOGA) for solving the optimization problem.

For estimating the yields from the PV plant, the 15 years hourly weather data between the years 2000 and 2014 was used. This large amount of data was handled by partitioning the yearly data into four seasons. The probability of solar PV power outputs was calculated by modeling the seasonal data using Beta Probability Density Function (Beta-PDF) and by generating a 24 hour solar curve for each season. The effectiveness of the proposed method was tested by adopting four time varying voltage dependent load models, which include the constant, industrial, residential and the commercial load models. The proposed method was tested on IEEE 33 bus and IEEE 69 bus test distribution networks. For investigating the impact of the BESS unit, two cases were considered. In the first case, the study considered the sizing and the utilization of the energy from the PV plant without the use of battery storage. In the second case, the study considered the sizing and the utilization of the energy from the Battery-Sourced Distributed Photovoltaic Generation (B-SDPVG). A conceptual PV-battery system also known as a Distributed Battery-Sourced Photovoltaic (DB-SPV) plant, tied to a distribution network is shown in FIGURE. 1 [18]. Moreover, the simulation code of the proposed algorithm is developed in MATLAB R2015a [44].

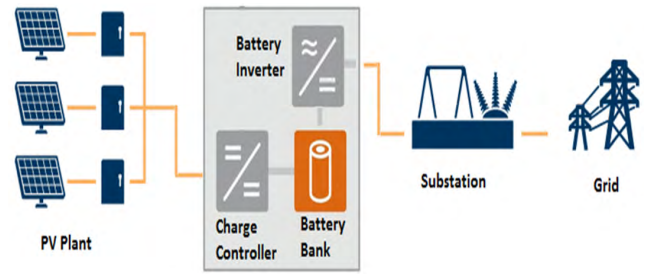


**FIGURE 1.** A typical battery-sourced distributed photovoltaic generation (B-SDPVG).

The structure of this paper is as follows. Section 2 covers the modeling of system parameters and thereby, the modeling of weather data, PV module power output, load flow equations, PV plant & B-SDPVG plant power outputs, and load models. Section 3 focuses on the problem formulations that include the mathematical expressions of total energy losses index (TELI), bus voltage deviations and the penetrations of the PV and the B-SDPVG plants. This section also addresses system and network constraints. Section 4 provides the explanation of the flowchart of the proposed algorithm and the control model for charging and discharging of batteries. In section 5, the simulation results are discussed in detail and are also provided in form of tables and graphical plots. Section 6 offers the conclusion of the work.

## II. MODELING OF THE SYSTEM PARAMETERS

### A. WEATHER DATA MODELING

The predictions of the outputs from the PV modules involve different modeling tools and algorithms [45]. These modeling tools analyze the weather data and predict the expected outputs of the PV modules by examining the variations in the weather data during the seasons. The Beta Probability Density Function (Beta-PDF) is a modeling tool, which has been used in many studies including the modeling of historical solar data [46]–[50]. Meteorological data has been primarily taken from the ground stations and satellites [51]. To serve the purpose of this research, the 15 year satellite weather data of the site at coordinates (29°19'25.6"N, 71°49'11.8"E) is acquired through the National Solar Radiation Database [52].

The historical weather data is handled by partitioning the yearly data into 4 seasons namely winter, spring, summer and autumn. Each season consists of the weather data of the following months, as provided in TABLE 1.

**TABLE 1.** Months of each season.

Season	Months
Winter	January, February & March
Spring	April, May & June
Summer	July, August & September
Autumn	October, November & December

The seasonal data is then modeled by using Beta Probability Density Function (Beta-PDF) and finally a 24 hour solar

curve is generated. The probability density function (pdf) of the beta distribution, for  $0 \leq s \leq 1$ , and shape parameters  $\alpha$ ,  $\beta > 0$ , for any hour can be expressed as

$$\text{beta}(s) = \begin{cases} \frac{\Gamma(\alpha + \beta)}{\Gamma(\alpha)\Gamma(\beta)} s^{\alpha-1} (1-s)^{\beta-1}, & 0 \leq s \leq 1, \alpha, \beta \geq 0 \\ 0 & \text{otherwise} \end{cases} \quad (1)$$

where,  $s$  is the irradiance of solar light in  $\text{kW/m}^2$  and  $\Gamma$  is the gamma function.  $\alpha$  and  $\beta$  are two shape parameters of the Beta-PDF, which are calculated with the help of Mean ( $\mu$ ) and Standard Deviation ( $\sigma$ ) of solar irradiance.  $\alpha$  and  $\beta$  can be calculated by

$$\beta = (1 - \mu) \left( \frac{\mu(1 + \mu)}{\sigma^2} - 1 \right) \quad (2)$$

$$\alpha = \frac{\mu X \beta}{1 - \mu}. \quad (3)$$

The probability of the solar irradiance state during any specific hour can be calculated as

$$p(s) = \int_{s1}^{s2} \text{beta}(s) ds \quad (4)$$

where  $s1$  and  $s2$  are the two solar irradiance limits, in which the probability of  $s$  has to be determined.

## B. OUTPUT FROM THE PV MODULE

The output of a PV module is measured in Watts. The characteristics of a PV module are generally provided in the form of following parameters [46], [48].

- $I_{sc}$  (Short circuit current in A)
- $V_{oc}$  (Open-circuit voltage in V)
- $IMPP$  (Current at maximum power point in A)
- $VMPP$  (Voltage at maximum power point in V)
- $NOCT$  (Nominal operating temperature of cell in  $^{\circ}\text{C}$ )
- $K_v$  (Voltage temperature coefficients in  $\text{V}/^{\circ}\text{C}$ )
- $K_i$  (Current temperature coefficients in  $\text{A}/^{\circ}\text{C}$ )

Moreover, the output of PV module for a given time segment ( $h$ ), can be measured by using

$$\begin{aligned} PV_{OUT}(h) &= \int_0^1 PV_{NETP}(s) ds \\ PV_{NET} &= FF \times V_{NET} \times I_{NET}, \\ FF &= \frac{V_{MPP} \times I_{MPP}}{V_{OC} \times I_{SC}} \\ V_{NET} &= V_{OC} - K_v \times T_C \\ I_{NET} &= s[I_{SC} + K_i \times (T_C - 25)] \\ T_C &= T_A + s \left( \frac{(NOCT - 20)}{0.8} \right) \end{aligned} \quad (5)$$

where,  $T_C$  and  $T_A$  are cell and ambient temperatures ( $^{\circ}\text{C}$ ), respectively, whereas the  $FF$  is known as fill factor.

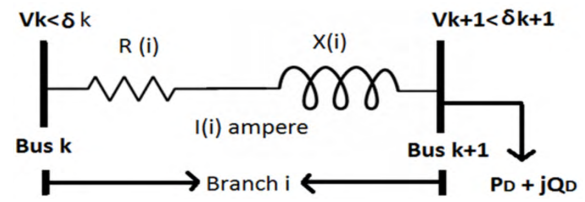


FIGURE 2. Two-bus section in a radial distributed network.

## C. POWER FLOW EQUATIONS

The load flow analysis in distribution networks is solved using Backward Forward Sweep Load Flow method [53].

The single line diagram of a section of a distribution network is presented in FIGURE. 2 which shows the two buses;  $k$  and  $k+1$ , connected through a branch line  $i$ . Resistance and reactance of the branch  $i$  are represented by  $R_i$  and  $X_i$ , respectively. Whereas,  $I(i)$  is the current that is flowing through the branch  $i$ . The power losses across the branch  $i$  can be calculated by

$$P_{loss(i)} = R(i) * \frac{P_{k+1}^2 + Q_{k+1}^2}{|V_{k+1}|^2}, \quad (6)$$

$$Q_{loss(i)} = X(i) * \frac{P_{k+1}^2 + Q_{k+1}^2}{|V_{k+1}|^2} \quad (7)$$

where,  $P_{loss(i)}$  and  $Q_{loss(i)}$  are the active and reactive power losses across the branch  $i$ . The total power losses in distribution network can be calculated by summing the active and reactive power losses of all the branches in the network. The total system losses can be calculated by

$$P_{loss\_total} = \sum_{i=1}^{no. \text{ of branches}} P_{loss(i)} + jQ_{loss(i)}. \quad (8)$$

## D. PV PLANTS MODEL

The output power from the solar PV plants can be used as a negative power load [54]. Assuming if the PV plant is going to be installed at bus  $k+1$ , then hourly total active and reactive power injections for bus  $k+1$  can be calculated using

$$P_{(i)}(t) = P_{(k+1),eff}(t) + P_{D(k+1)}(t) + P_{loss(i)}(t) - P_{PV}(t) \quad (9)$$

$$Q_{(i)}(t) = Q_{(k+1),eff}(t) + Q_{D(k+1)}(t) + Q_{loss(i)}(t) - Q_{PV}(t). \quad (10)$$

Since  $Q_{PV}$  is a function of  $P_{PV}$  with a fixed power factor, therefore,

$$Q_{PV} = aP_{PV}$$

and,

$$a = \pm \tan(\cos^{-1}(pf(P_{PV}))).$$

When  $\text{sign} = +1$ : the inverter is injecting reactive power,  $\text{sign} = -1$ : the inverter is consuming reactive power, where  $pf$  is the operating power factor of the inverter. With no reactive power capability, the power factor of solar PV inverter will



be unity. After connecting PV plant, the new power losses across the branch  $i$  can be calculated by using

$$P_{loss(i)}^{PV} = R_{(i)} * \frac{(P_{k+1} - P_{PV})^2 + (Q_{k+1} - Q_{PV})^2}{|V_{k+1}|^2} \quad (11)$$

$$Q_{loss(i)}^{PV} = X_{(i)} * \frac{(P_{k+1} - P_{PV})^2 + (Q_{k+1} - Q_{PV})^2}{|V_{k+1}|^2}. \quad (12)$$

Similarly, the total power losses with the addition of PV plant is given by

$$P_{loss\_total}^{PV} = \sum_{i=1}^{no. of branches} P_{loss(i)}^{PV} + jQ_{loss(i)}^{PV}. \quad (13)$$

The conversion efficiencies and performance of the inverters highly affect the overall system operation and outputs of PV modules. Inverters are normally chosen based on the rating of system demand or maximum outputs that a solar PV plant can produce. The typical inverter's conversion efficiency curve as provided in [55] indicates that the inverter's conversion efficiency from DC-to-AC is not constant and this efficiency is less if the input DC power from solar PV modules is less than the rated DC values of inverter. In such case, the size of inverter should also be chosen based on predicted yields from PV plants. However, the size of the inverters in this study is considered 120% of the maximum power that the solar PV plant can produce under the optimum PV plant size. The typical inverter's conversion efficiency curve as provided in [55] was used for the simulation works of this study.

### E. BATTERY-SOURCED DISTRIBUTED PV GENERATION (B-SDPVG) MODEL

The rationale behind developing the Battery-Sourced Distributed PV Generation (B-SDPVG) is to convert the non-dispatchable PV plants into dispatchable generator [56]. The B-SDPVG is considered as reliable source of energy; the output power from batteries can be adjusted according to the energy demand and according to the availability of the energy, stored in the batteries. Moreover, the inverters with battery backup are capable of injecting or absorbing the reactive power, and the power factor of the battery inverters can be adjusted according to the system requirements [57].

Similar to the solar PV plants, output power from the Battery-Sourced Distributed Photovoltaic Generation (B-SDPVG) plant was used as negative load. Batteries were charged only from the electricity, produced through the solar PV plant to avoid putting additional burden on existing generators. Since the charging of the batteries is done through the PV plant itself, the grid will not experience any change in terms of power flow, when the batteries are being charged. The changes in the flow of power will occur only during the followings cases:

- Grid is being supplied with the power from the PV plant
- Grid is being supplied with the power by discharging the batteries.

Assuming that the B-SDPVG plant will be installed at bus  $k+1$ , depending on the output of B-SDPVG plant, the hourly

total active and reactive power injections for bus  $k+1$  are given by

$$P_{(i)}(t) = P_{(k+1),eff}(t) + P_{D(k+1)}(t) + P_{loss(i)}(t) - P_{B-SDPVG}(t) \quad (14)$$

$$Q_{(i)}(t) = Q_{(k+1),eff}(t) + Q_{D(k+1)}(t) + Q_{loss(i)}(t) - Q_{B-SDPVG}(t). \quad (15)$$

Since  $Q_{PV}$  is a function of  $P_{PV}$  with a fixed power factor, therefore,

$$Q_{PV} = aP_{B-SDPVG}$$

and,

$$a = \pm \tan(\cos^{-1}(pf(P_{B-SDPVG}))).$$

Since most studies in literature have considered the supplying of active power only, the inverter used for B-SDPVG plant in this study shall have a unity power factor. After connecting B-SDPVG plant, the new power losses across the branch  $i$  can be calculated using

$$P_{loss(i)}^{B-SDPVG} = R_{(i)} * \frac{(P_{k+1} - P_{B-SDPVG})^2 + (Q_{k+1} - Q_{B-SDPVG})^2}{|V_{k+1}|^2} \quad (16)$$

$$Q_{loss(i)}^{B-SDPVG} = X_{(i)} * \frac{(P_{k+1} - P_{B-SDPVG})^2 + (Q_{k+1} - Q_{B-SDPVG})^2}{|V_{k+1}|^2}. \quad (17)$$

Similarly, the total power losses with the addition of B-SDPVG plant is calculated by

$$P_{loss\_total}^{B-SDPVG} = \sum_{i=1}^{no. of branches} P_{loss(i)}^{B-SDPVG} + jQ_{loss(i)}^{B-SDPVG}. \quad (18)$$

### F. LOAD MODELS

In practical distribution networks, the load can be classified as constant, industrial, residential and commercial load [48]. These types of loads are also referred to as voltage-dependent load models. Depending on the type of loads, the new loads  $P_{Dnew}$  for each bus are calculated using

$$P_{Dnew(k)} = P_{Da(k)} * V_{(k)}^{v\alpha} \quad (19)$$

$$Q_{Dnew(k)} = Q_{Da(k)} * V_{(k)}^{vr}. \quad (20)$$

where,  $P_{Da}$  and  $Q_{Da}$  are the actual active and reactive loads connected at bus  $k$ , and  $V(k)$  is the voltage magnitude of  $k^{th}$  bus which is calculated under the base load conditions. The two parameters  $v\alpha$  and  $vr$  are known as voltage coefficients for active and reactive power loads. The values of  $v\alpha$  and  $vr$  are provided in TABLE 2.

Similarly, the hourly total loads of the network can be calculated as

$$P_{DTotal}(t) = \sum_{k=2}^{number of buses} P_{Dnew(k)}(t), \quad (21)$$

$$Q_{DTotal}(t) = \sum_{k=2}^{number of buses} Q_{Dnew(k)}(t). \quad (22)$$

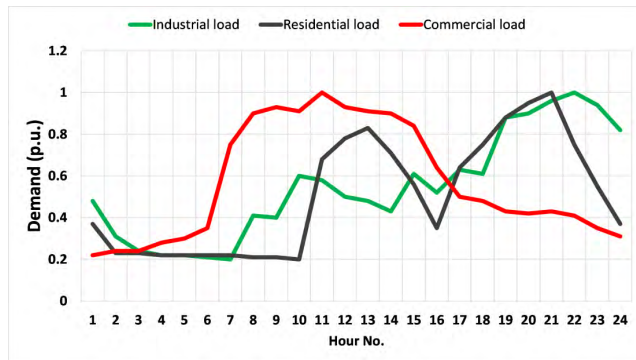
**TABLE 2.** Voltage coefficients for active and reactive power loads.

Type of load	$v\alpha$	$vr$
Constant	0	0
Industrial	0.18	6.00
Residential	0.92	4.04
Commercial	1.51	3.40

The daily demand curves for each load model are provided in FIGURE 3. The logic behind using the time varying voltage dependent load models is because the output from PV plant is also time varying. For each season, the study considers the seasonal time variations in load as provided by IEEE-RTS load data in [58]. The new loads of the time varying load models can be calculated using the equations (19) and (20) and mathematically can be expressed as

$$P_{Dnew(k)}(t) = P_{Da(k)}(t) * V_{(k)}^{v\alpha}(t) \quad (23)$$

$$Q_{Dnew(k)}(t) = Q_{Da(k)}(t) * V_{(k)}^{vr}(t). \quad (24)$$

**FIGURE 3.** Daily demand curves for loads under study.

### III. PROBLEM FORMULATION

The objective function of this study is to minimize total energy losses in the distribution networks. The optimization problem is solved by determining the optimum size of PV plant and BESS and their locations. To avoid the additional losses, BESS are connected at the same bus with PV plant. The remaining optimizing parameters are BESS capacity, optimum level of energy (OpE) that can be supplied and lastly the level of load which is used for the charging and discharging of batteries.

The amount of BESS is considered as a percentage of the total size of the PV plant. Since the cost of battery is comparatively high, therefore, the maximum size for the BESS considered in this study is 200% of the size of the PV plant. For example, for a 1 MW<sub>p</sub> PV plant, the maximum BESS size shall be 2 MWh. The size of BESS will optimally be chosen ranging between 0 to maximum size of BESS.

Moreover, rather than supplying of power equal to demand, the dispatch from B-SDPVG plants during each hour shall be

done by using the value of OpE. The OpE value will also be used for the charging and discharging of the batteries. For example, the batteries would be considered charged if the amount of the power from PV plants during the time (t) is higher than the OpE (t). Similarly, batteries would be considered discharged if the energy available at BESS during the time (t) is enough to provide the energy equal to OpE (t).

Furthermore, unlike the previous studies; when batteries were charged only when output from the PV plants was higher than demand, and batteries were discharged due to the economic reasons i.e time-of-use (ToU).

The choice for charging and discharging of batteries in this study is intended to provide technical benefits to the distribution networks. For determining the time of the charging and discharging of the batteries, a level of the hourly load (percentage of the peak load) shall be used. For making the decision whether to charge or to discharge the batteries, the control model for BESS will verify the load level on hourly basis. For example, batteries during the time (t) will only be considered to discharge the batteries if the load during the time (t) is greater than 50 % of the peak load. In other case, the batteries shall be considered for the charging operations. The yearly total system losses for base case study can be obtained using

$$P_{loss\_total}(t) = 365 * \sum_{i=1}^{no. of branches} P_{loss(i)}(t) + jQ_{loss(i)}(t).$$

Meanwhile, the total energy losses with the addition of PV plant is given by

$$P_{loss\_total}^{PV}(t) = 365 * \sum_{i=1}^{no. of branches} P_{loss(i)}^{PV}(t) + jQ_{loss(i)}^{PV}(t). \quad (25)$$

Similarly, the total energy losses with the addition of B-SDPVG, can be calculated by using

$$P_{loss\_total}^{B-SDPVG}(t) = 365 * \sum_{i=1}^{no. of branches} P_{loss(i)}^{B-SDPVG}(t) + jQ_{loss(i)}^{B-SDPVG}(t). \quad (26)$$

The deviations in network losses due to the installation of DG (say B-SDPVG) can be calculated by dividing equation (26) with equation (25). This method is termed as total energy losses Index (TELI) and is expressed as following.

$$Total Energy loss index (TELI) = \sum \frac{real(P_{DG_{loss\_total}}(t))}{real(P_{loss\_total}(t))} \quad (27)$$

The main objective of this study is to minimize the total energy losses in distribution networks, which can be achieved by the minimization the total energy loss index in this study. This can be expressed as following.

$$f = minimize Total Energy Loss Index (TELI) \quad (28)$$

The changes in bus voltage magnitude are measured as the voltage deviations [59]. The deviation in voltages of each bus

during the time (t) can be calculated using

$$VDev_k(t) = |1 - V_k|^2(t). \quad (29)$$

The bus with maximum voltage deviation shall indicate the status of whole network. The maximum voltage deviation ( $VDev_{max}$ ) from a time varying voltage dependent load model can be calculated using the following equation.

$$VDev_{max} = \max(|1 - V_k|^2(t)) \quad (30)$$

The penetration level of the PV plant is known as the ratio of total energy supplied by the PV plant and the total energy consumption of the network [20]. For a DG (say PV only or B-SDPVG) plant, the penetration level of the plant is given by

$$PVpenetration(\%) = \frac{\sum_{t=1}^{96} P_{DG}(t)}{\sum_{t=1}^{96} P_{DTotal}(t)} * 100. \quad (31)$$

Moreover, for the simulation, following constraints are considered.

#### A. CONSTRAINTS

##### 1) DISTRIBUTED GENERATION CAPACITY

$$P_{DG}^{min} < P_{DG} < P_{DG}^{max} \quad (32)$$

where,  $P_{DG}^{min}$  is equal to 0 and  $P_{DG}^{max}$  is equal to a fraction of the peak active power load of each voltage-dependent load. Therefore,  $P_{DG}^{max}$  for each type of load type will not be the same.

##### 2) BESS CAPACITY

$$0 < BESS < P_{DG}^{max} * \text{daily energy yields from PV plants} \quad (33)$$

##### 3) OPTIMUM ENERGY LEVELS (OPE)

$$0 < OpE < 100\% \quad (34)$$

##### 4) LOAD LEVEL ( $L_{LEVEL}$ ) FOR THE CHARGE/DISCHARGE OF BESS

$$0 < L_{level} < 100\% \text{ of peak load}$$

##### 5) NETWORK POWER BALANCE

$$P_{substation}(t) + P_{DG}(t) = P_{DTotal}(t) + P_{loss\_total}(t) \quad (35)$$

$$Q_{substation}(t) + Q_{DG}(t) = Q_{DTotal}(t) + Q_{loss\_Total}(t) \quad (36)$$

where,  $P_{substation}$  and  $Q_{substation}$ , are respectively the active and reactive power supplies to distribution network from the substation.

##### 6) DG PLACEMENT

The bus no.1 in the distributed network is considered as slack bus, therefore, the DGs can be connected to any bus excluding the bus no.1.

$$2 \leq DG_{location} \leq \max(\text{number of buses}) \quad (37)$$

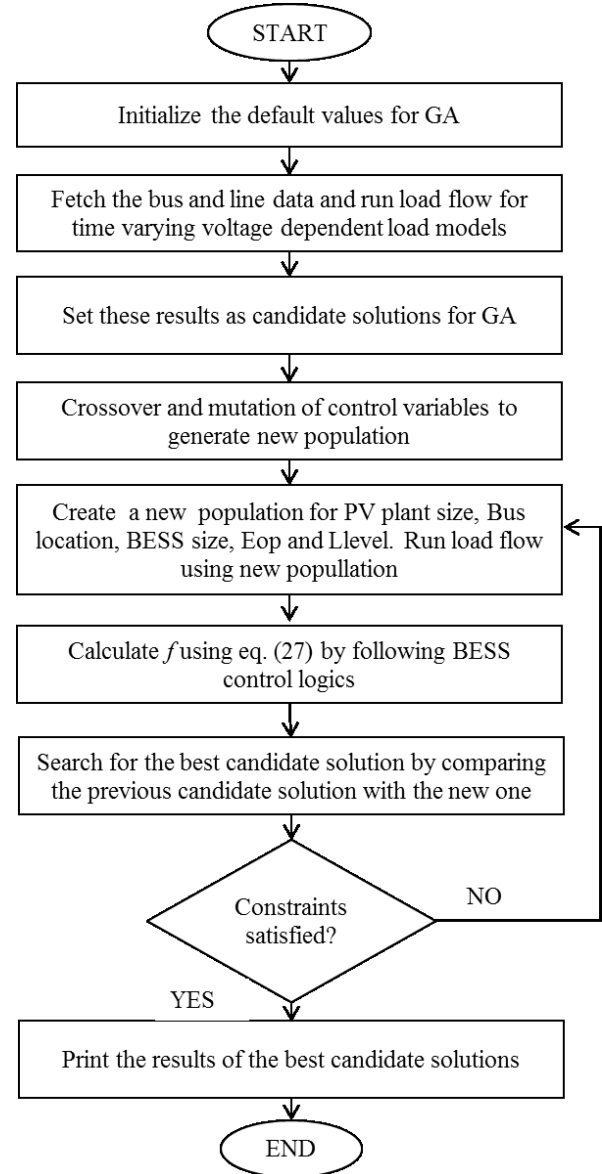


FIGURE 4. Flowchart of Genetic Algorithm for solar PV and B-SDPVG sizing and placement simulation results.

##### 7) BUS VOLTAGE LIMITS

$$V_{min} \leq V \leq V_{max} \quad (38)$$

In order to maintain the power quality of distribution network, the bus voltage magnitude will remain below the 1.0 p.u.

#### IV. OPTIMIZATION METHOD

The Genetic Algorithm (GA) is a programming optimization technique to solve constrained and unconstrained problems. Inspired by Darwinian's principle, to solve the real-world problem, this optimization technique follows biological growth process. GA optimizes by using an evolution and a natural selection. GA consists of a data structure similar to chromosomes and these chromosomes are changed by using

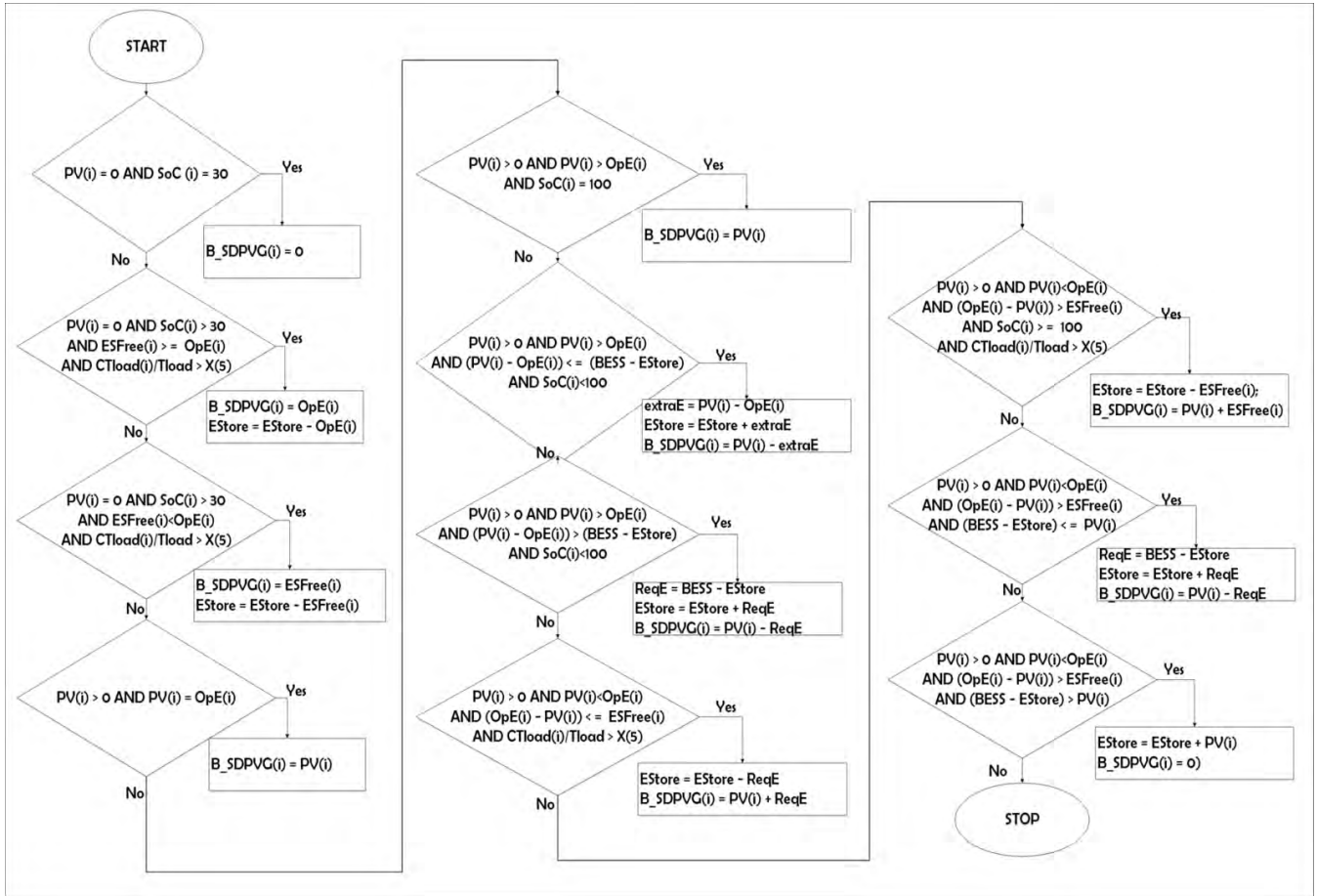


FIGURE 5. Logic control model for the charging and discharging of the batteries of B-SDPVG.

TABLE 3. Summary of seasonal weather data.

Hour No.	Winter		Spring		Summer		Autumn	
	$\mu$	$\sigma$	$\mu$	$\sigma$	$\mu$	$\sigma$	$\mu$	$\sigma$
9	0.01	0.02	0.12	0.03	0.08	0.02	0.02	0.02
10	0.14	0.06	0.32	0.04	0.25	0.05	0.18	0.06
11	0.35	0.08	0.53	0.06	0.42	0.09	0.38	0.07
12	0.54	0.10	0.71	0.08	0.57	0.13	0.55	0.08
13	0.69	0.12	0.84	0.09	0.68	0.17	0.67	0.09
14	0.77	0.12	0.91	0.10	0.75	0.19	0.73	0.09
15	0.78	0.13	0.92	0.08	0.76	0.18	0.71	0.09
16	0.72	0.12	0.85	0.08	0.70	0.18	0.63	0.09
17	0.60	0.11	0.72	0.08	0.58	0.15	0.49	0.07
18	0.42	0.09	0.54	0.06	0.43	0.11	0.30	0.06
19	0.21	0.07	0.33	0.04	0.25	0.07	0.09	0.04
20	0.03	0.03	0.11	0.03	0.08	0.04	0.00	0.00

selection, crossover and mutation operators. The details of working mechanism of GA and functions of its parameters are provided in [25].

The Genetic Algorithm (GA) is also capable of solving problems if the unknown value is integer. Since the location of the DG in distribution network is actually the number of a bus, whereas the size is a percentage of system's peak demand. The mix of DG location as integer and DG size as non-integer creates a need of optimization of mixed integer variables. In order to solve this, Mixed Integer Optimization using

Genetic Algorithm (MIOGA) is adopted. The optimization process flowchart of the proposed algorithm is provided in FIGURE. 4, whereas, the logic control model for the charging and discharging of the batteries of B-SDPVG are provided in FIGURE. 5.

## V. SIMULATION RESULTS AND DISCUSSIONS

From the seasonal mean ( $\text{kW/m}^2$ ) and the standard deviation ( $\text{kW/m}^2$ ) of the historical solar irradiance data, the values for seasonal beta ( $\beta$ ) & alpha ( $\alpha$ ) are calculated by using



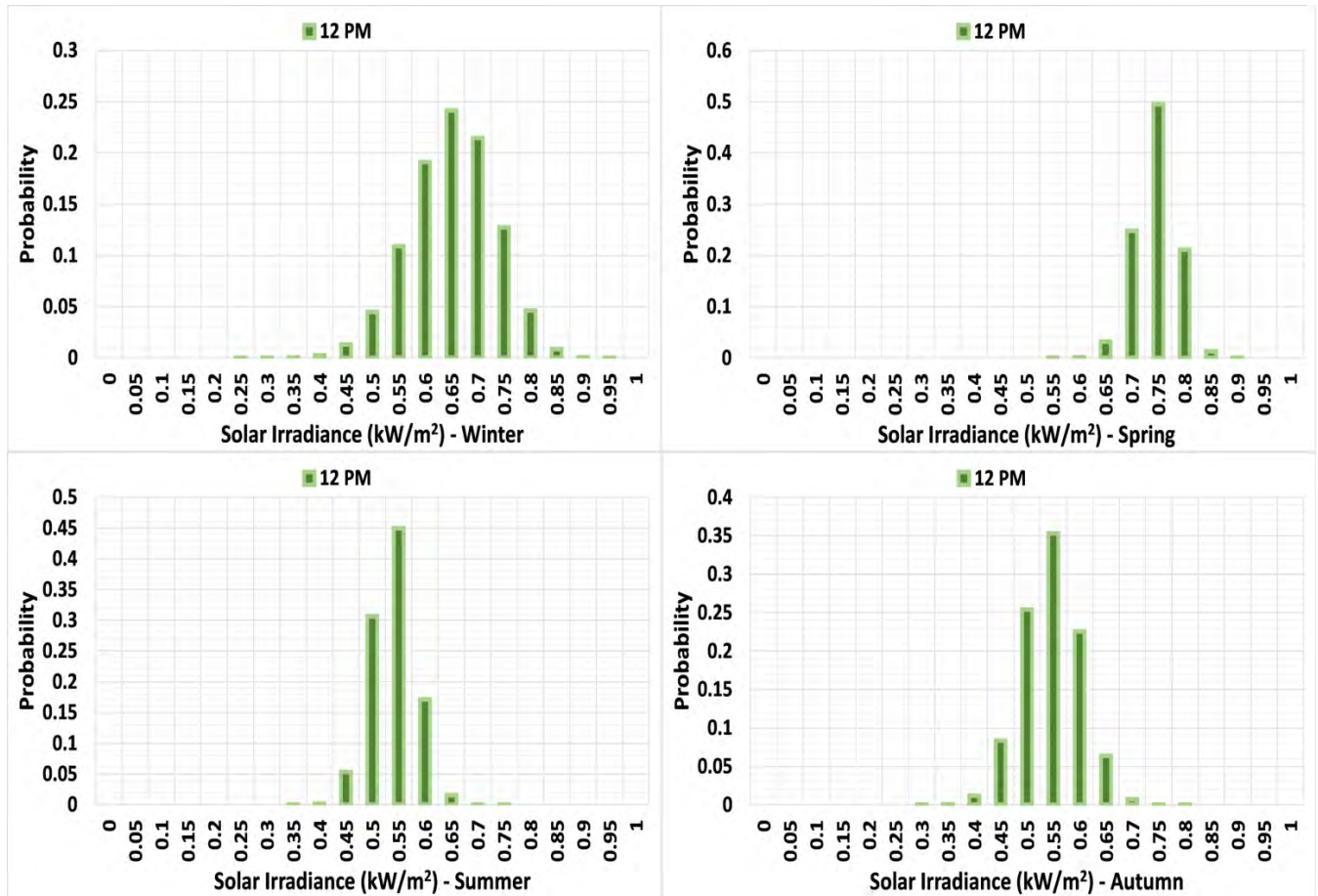


FIGURE 6. Probability density functions (PDFs) of solar irradiance.

TABLE 4. Specifications of the photovoltaic (PV) module.

DESCRIPTION	Value
Nominal Operating Temperature Of Cell (NOCT)	44 °C
Current at Maximum Power Point (IMPP)	8.28 A
Voltage at Maximum Power Point (VMPP)	30.2 V
Short-Circuit Current (ISC)	8.7 A
Open-Circuit Voltage (VOC)	37.6 V
Current Temperature Coefficients (Ki)	0.0045 A/°C
Voltage Temperature Coefficients (Kv)	0.1241 V/°C

equations (2) and (3) and are provided in TABLE 3. The hourly Probability Density Functions (PDFs) for 12 pm for each season are calculated by using equations (1) and (4) and are plotted in FIGURE. 6.

The ambient temperature is the average of the seasonal hourly 15 years temperature data. The yearly temperature of the site is ranging in between 12 °C – 45 °C. The minimum and maximum temperature during the each season is 12 & 29 °C, 29 & 45 °C, 29 & 40 °C, and 16 & 32 °C, for winter, spring, summer and autumn, respectively.

Based on the seasonal PDF values, seasonal irradiances and seasonal ambient temperature, the expected seasonal daily solar PV outputs are calculated by using equation (5).

From the expected seasonal daily solar PV outputs, it is known that this site has maximum irradiation of 907 Watts/m<sup>2</sup> during the summer time. On average, the site receives 4.4 to 6.9 peaks sunny hours (PSH). By, using the specifications as provided in TABLE 4, the maximum output that the PV module can produce is 177 watts during the spring time.

The proposed algorithm was simulated and applied on IEEE 33 bus and IEEE 69 bus test distribution networks. The active and reactive demands of IEEE 33 bus network are 3715 kW & 2300 kVAr, whereas, the active and reactive demands of IEEE 69 bus network are 3800 kW & 2690 kVAr. The total base case real and reactive power losses for IEEE 33 bus are 211 kW & 143 kVAr, whereas the total base case real and reactive power losses for IEEE 69 bus are 225 kW & 102 kVAr [60]–[62]. The single line diagrams, line and load data of both distribution networks are presented in [63]. The first bus in the radial distribution networks is slack bus, which implies that this bus cannot be used for placing the DG units. Therefore, the DG units can be considered suitable to be installed at any bus from 2 to 33 in IEEE 33 bus system and from 2 to 69 in IEEE 69 bus system. For both test cases, four types of time varying voltage-dependent

**TABLE 5.** Summary of results with PV only in IEEE 33 bus test system.

Parameters	Constant		Industrial		Residential		Commercial	
	Without	With PV	Without	With PV	Without	With PV	Without	With PV
PV size (MW)@Bus No		3.3@6		2.85@6		3.15@6		3.77@6
Yearly Energy Losses (MWh)	586.34	455.66	633.63	538.00	528.17	409.60	593.99	422.65
Reduction in Energy Losses		22.29 %		15.09 %		22.45 %		28.85 %
DG Penetration		34.46 %		27.57 %		33.91 %		36.81 %
Voltage Deviation	0.183	0.183	0.180	0.180	0.169	0.169	0.161	0.144

**TABLE 6.** Summary of results with PV only in IEEE 69 bus test system.

Parameters	Constant		Industrial		Residential		Commercial	
	Without	With PV	Without	With PV	Without	With PV	Without	With PV
PV size (MW)@Bus No		2.44@61		2.11@61		2.3@61		2.72@61
Yearly Energy Losses (MWh)	622.57	436.07	671.21	535.37	554.06	388.17	617.94	383.13
Reduction in Energy Losses (%)		29.96		20.24		29.94		38.00
DG Penetration (%)		24.82		19.92		24.16		25.83
Voltage Deviation	0.173	0.173	0.171	0.171	0.160	0.160	0.151	0.133

**TABLE 7.** Summary of results with B-SDPVG for each load model in IEEE 33 bus network.

Parameters	Constant		Industrial		Residential		Commercial	
	Without	With PV-BESS	Without	With PV-BESS	Without	With PV-ESS	Without	With PV-ESS
PV size (MW)@Bus No		5.14@6		5@6		4.7@6		5.1@6
Total BESS Size (MWh)		10.28		10.00		9.40		10.19
Yearly Energy Losses (MWh)	586.34	354.57	633.63	424.61	528.17	317.08	593.99	397.18
Reduction in Energy Losses (%)		39.53		32.99		39.97		33.13
DG Penetration (%)		51.42		47.14		50.96		44.85
Voltage Deviation	0.183	0.117	0.180	0.138	0.169	0.103	0.161	0.151

**TABLE 8.** Summary of results with B-SDPVG for each load model in IEEE 69 bus network.

Parameters	Constant		Industrial		Residential		Commercial	
	Without	With PV-BESS	Without	With PV-BESS	Without	With PV-ESS	Without	With PV-ESS
PV size (MW)@Bus No		3.76@61		3.71@61		3.41@61		3.61@61
Total BESS Size (MWh)		7.52		7.42		6.82		7.22
Yearly Energy Losses (MWh)	622.57	287.26	671.21	371.01	554.06	260.86	617.94	356.53
Reduction in Energy Losses (%)		53.86		44.72		52.92		42.30
DG Penetration (%)		36.73		34.17		35.92		30.11
Voltage Deviation	0.173	0.093	0.171	0.091	0.160	0.090	0.151	0.142

load models have been used. These load models include constant, industrial, residential and commercial loads. The four time varying loads are modeled by using the

equations (23) and (24). The constraints for the simulations for both test networks are kept the same as described earlier.

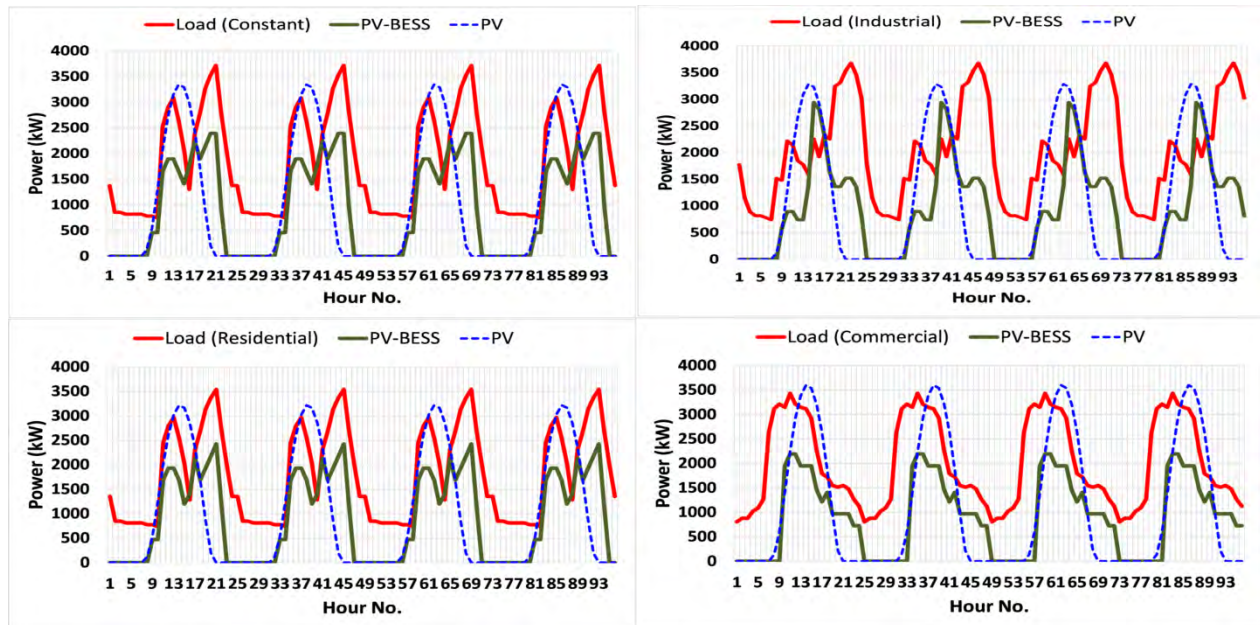


FIGURE 7. Hourly power demand and output from PV plant with and without BESS in IEEE 33 bus distribution network.

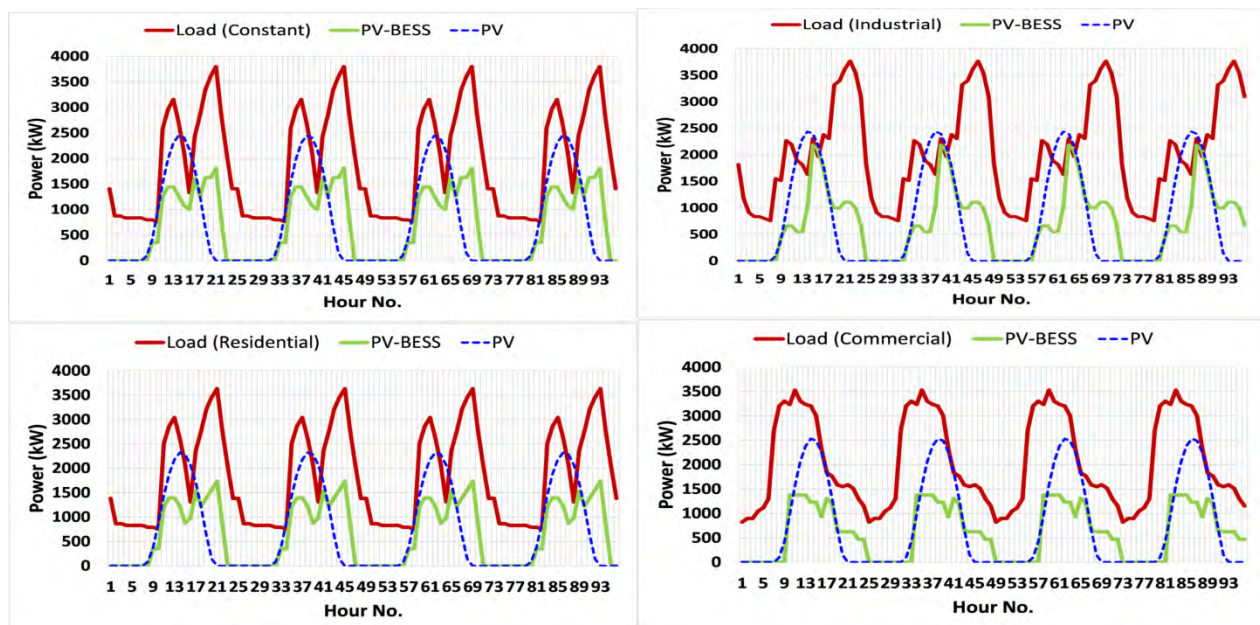


FIGURE 8. Hourly power demand and output from PV plant with and without BESS in IEEE 69 bus distribution network.

In [64], the efficiency of the battery charging and discharging is regarded as round trip and for which the value ranges between 80 % to 99%. However, this study considers two separate efficiency curves for the charging and discharging of the batteries as provided in [55] and [65], respectively.

State-of-charge (SoC) is an indicator of the energy stored in the batteries. Accurate measurements for SoC are essential, as in addition to estimation of available energy, it also determines the health and age of the batteries [14]. In that regard,

state estimation algorithms for battery systems that monitor the internal states in real-time have been proposed [66]. The state-of-charge (SoC) of the batteries is tracked on hourly basis. On first hour, it is assumed that the batteries are pre-charged and are having the minimum SoC of 30 %. Using the SoC, the amount of energy from BESS that can be used for the grid is calculated. SoC for the remaining hours throughout the simulation will depend on the energy available through the charging from PV power and discharging of the batteries



**TABLE 9.** Summary of the yearly energy losses (MWh) in 33 bus distribution network.

Load Type	Without	With PV	With PV-BESS
Constant	586.34	455.66	354.57
Industrial	633.63	538.00	424.61
Residential	528.17	409.60	317.08
Commercial	593.99	422.65	397.18

**TABLE 10.** Summary of the yearly energy losses (MWh) in 69 bus distribution network.

Load Type	Without	With PV	With PV-BESS
Constant	622.57	436.07	287.26
Industrial	671.21	535.37	371.01
Residential	554.06	388.17	260.86
Commercial	617.94	383.13	356.53

for the grid. For investigating the impact of BESS, two cases are considered; PV plant without BESS and PV plant with BESS.

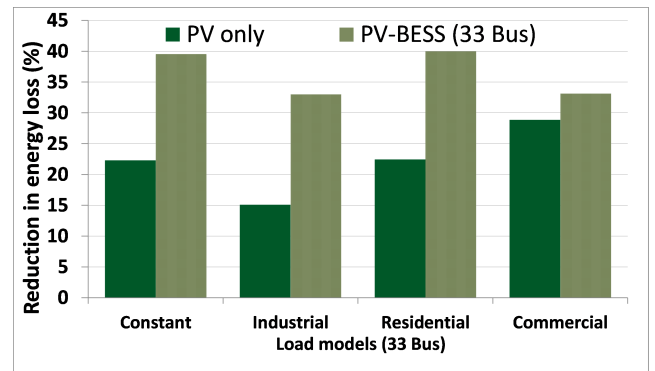
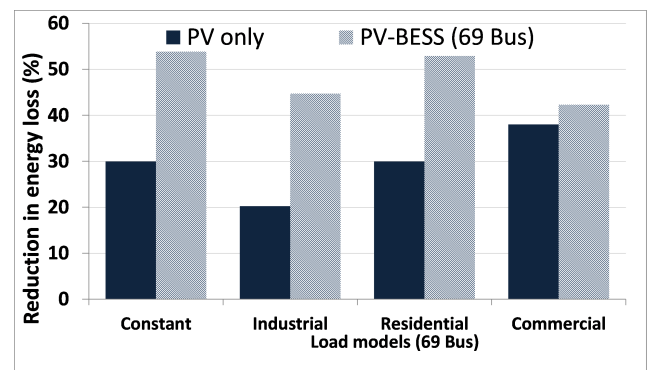
*Case A) PV Plant Without Bess:* The simulation results of size and placement of PV plant and BESS unit, the reduction in real power losses, voltage deviations and the penetration of the PV plant in IEEE 33 bus and IEEE 69 bus test distribution networks are provided in TABLE 5 and TABLE 6.

Due to the difference of energy consumptions, the size of PV plants for each load model in both distribution networks is not the same. The locations of PV plant in IEEE 33 bus and IEEE 69 bus distribution networks are the bus no.6 and bus no.61. Among the four load models, PV plants in both distribution networks are considered favorable for commercial load models due to lower energy losses, higher penetration levels and improved bus voltage profiles. This is mainly because the daily load curve of commercial load model fits into the daily PV output curve of the PV plant.

The improvement in bus with lowest voltage due to the installation of PV plant in both distribution networks was only noticeable for the commercial load. This was mainly because the peak loads in the other load models occurred during the off sunny hours of the day. The rates of reduction in total energy losses in IEEE 33 bus and IEEE 69 bus network were ranging in between 15 % to 29 % and 20% to 38 %, respectively.

*Case B) PV Plant With Bess:* The simulation results for the B-SDPVG plant, the reduction in real power losses, voltage deviations and the penetration of B-SDPVG plant power in IEEE 33 bus and IEEE 69 bus test distribution networks are summarized in TABLE 7 and TABLE 8.

As compared to the previous case, the rate of reduction in total energy losses in each load model due to the addition of BESS units in both distribution networks were significantly higher. Due to the increased sizes of PV plants, the reduction rates in energy losses, enhancements in bus voltage profiles

**FIGURE 9.** The reduction in energy losses with PV and PV-BESS in IEEE 33 bus network.**FIGURE 10.** The reduction in energy losses with PV and PV-BESS in IEEE 69 bus network.

and increments in the penetration levels in each load model were also noticed. The installation of BESS units did not found to affect the locations of PV plants. The locations of B-SDPVG plants in IEEE 33 bus and IEEE 69 bus distribution networks are the bus no.6 and the bus no. 61, respectively. The rates of increments in the sizes of the PV plants and the rates of reductions in network were found to be linear in most of the time varying voltage-dependent load model. The hourly power demand and outputs from the PV plants with and without batteries for each load model in IEEE 33 bus and IEEE 69 are plotted in FIGURE. 7 and FIGURE. 8.

Furthermore, the impact of adding the BESS unit in the distribution network was investigated by comparing the results of B-SDPVG with the results of first case (PV only). The comparison of the two cases was done in terms of the supply of power during the peak loads, reductions in network losses, improvements in bus voltage deviations and changes in the penetrations levels for load model.

#### A. POWER SUPPLY DURING PEAK LOADS

The PV plants without the battery storage were found to be capable of providing the supply of power during the peak load for commercial load only. This was mainly due to the peak loads in constant, industrial and residential loads appeared at hour 21 and hour 22, at night time. The rate of power losses in



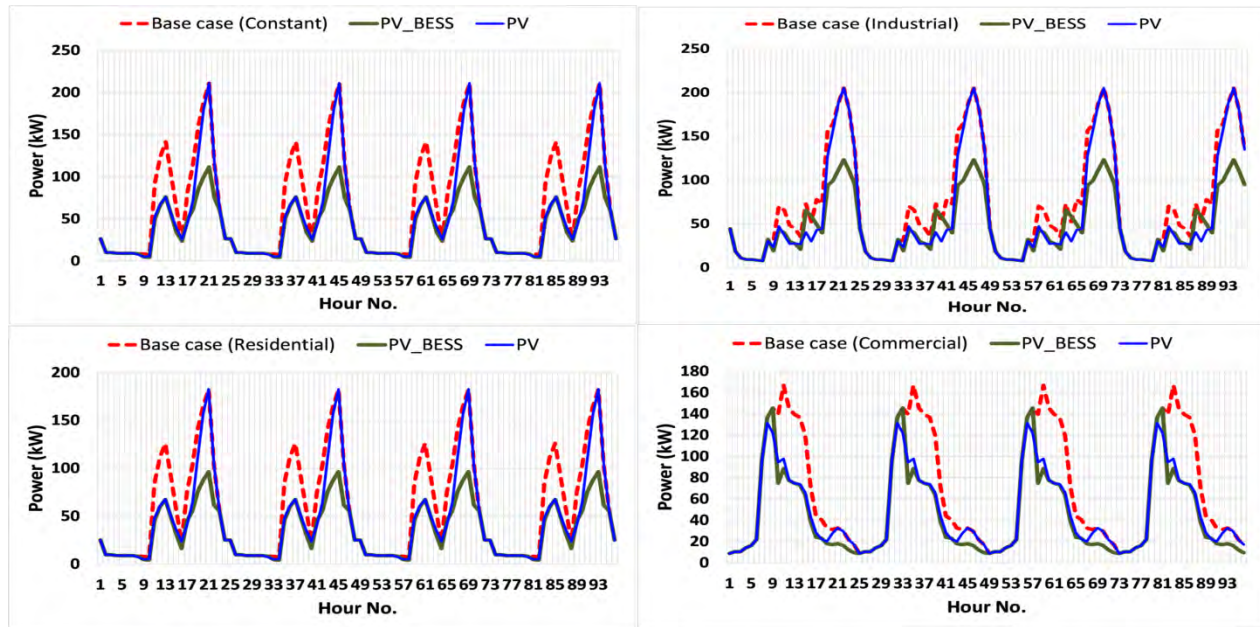


FIGURE 11. Hourly power losses with and without BESS in IEEE 33bus distribution network.

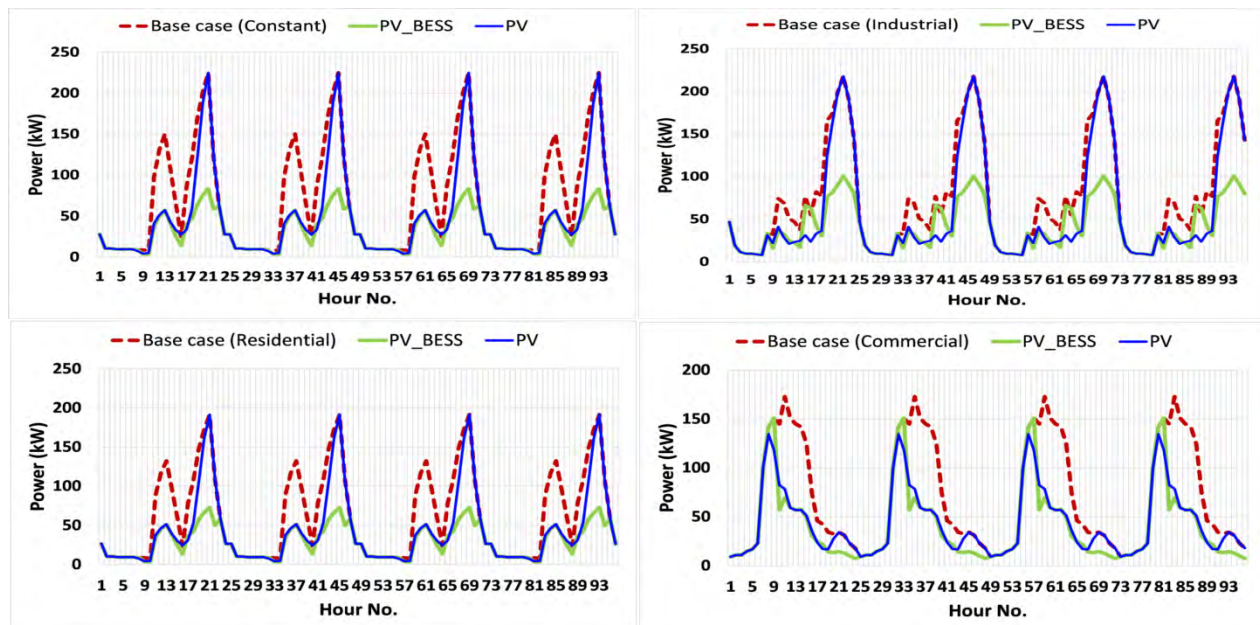


FIGURE 12. Hourly power losses with and without BESS in IEEE 69bus distribution network.

the network depends on the level of the loads which could be an interesting outcome. Therefore, it could be concluded that the PV plants lonely cannot supply the power during the hours when network can encounter the maximum amount of energy losses. In the case of BESS, the supply of power during the peak load hours was observed for each load model. Therefore, it can be concluded that B-SDPVG can provide sufficient amount of energy during the non-sunny hours, and this way a huge amount of energy losses is reduced.

## B. IMPACT ON ENERGY LOSSES

The scheduling of output power from B-SDPVG plant in each load model was done by optimum scheduling of charging and discharging of battery storage. The optimization of scheduling of charging and discharging of battery storage during the simulation was done to reduce the total energy losses in the network. The network power losses without and with battery storage in IEEE 33 bus network during the peak load hours were 210.99 kW & 111.57 kW, 205.07 & 123.15,

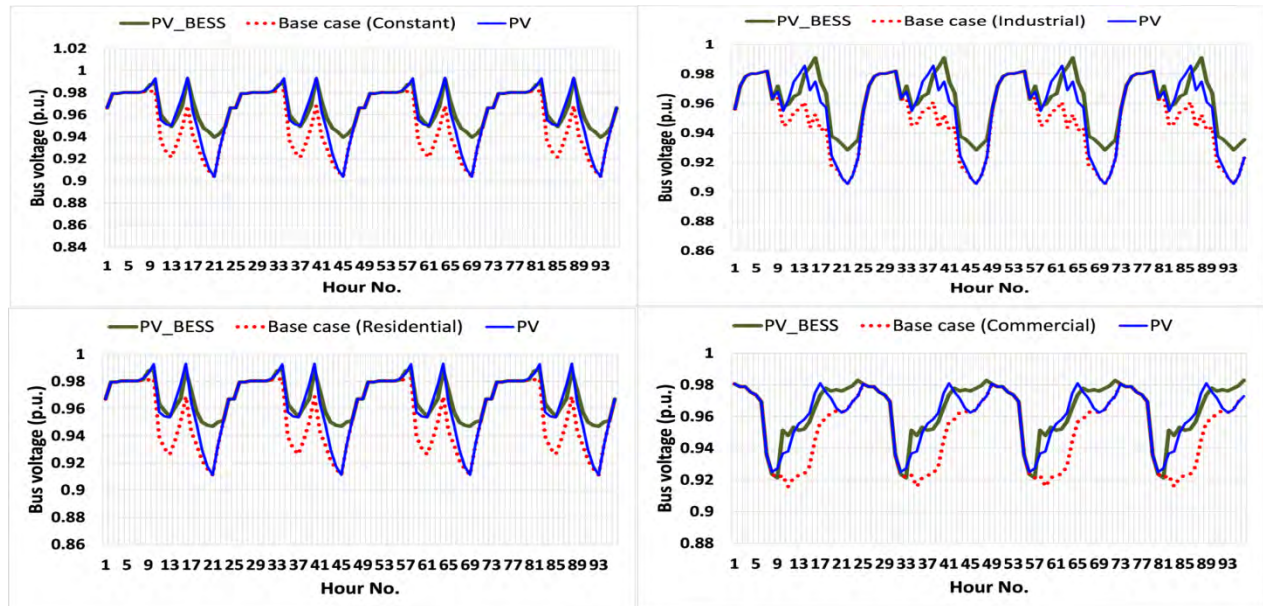


FIGURE 13. The voltage magnitudes of weakest bus with and without BESS in IEEE 33 bus distribution network.

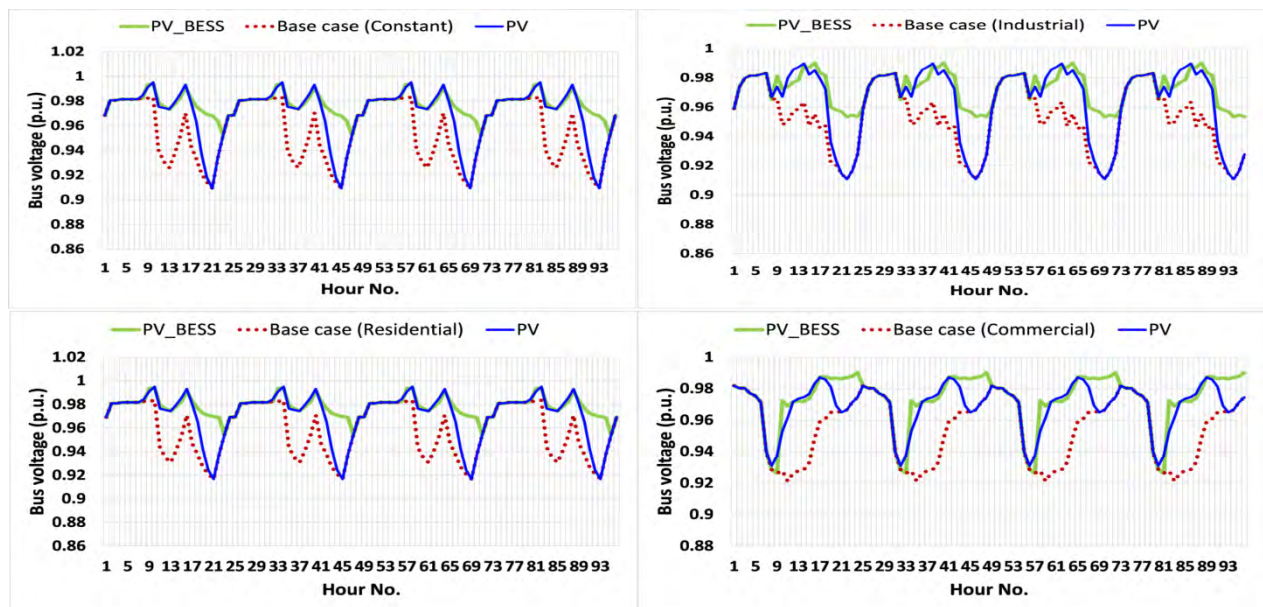


FIGURE 14. The voltage magnitudes of weakest bus with and without BESS in IEEE 69 bus distribution network.

182.6 kW & 96.5 kW and 166.67 & 88.5 kW, in constant, industrial, residential and commercial load models, respectively.

Similarly, the network power losses without and with battery storage in IEEE 69 bus network during the peak load hours were 224.94 kW & 83.32 kW, 217.88 kW & 100.74 kW, 191.37 kW & 72.72 kW and 172.74 kW & 69.24 kW, in constant, industrial, residential and commercial load models, respectively.

After the addition of B-SDPVG plant, the rate of reduction in total energy losses in IEEE 33 bus distribution network was

ranging in between 33 % to 40 %. Similarly, the reduction in total energy in IEEE 69 bus distribution network was ranging in between 42 % to 54 %. The total energy losses in base case, with PV only and with B-SDPVG plant for constant & industrial, residential and commercial load models, in IEEE 33 and IEEE 69 bus distribution networks are summarized in TABLE 9 and TABLE 10, respectively.

Results show that BESS units have greatly contributed in reducing the amount of the total energy losses for each time varying voltage dependent load model in both distribution networks. The introduction of BESS units in



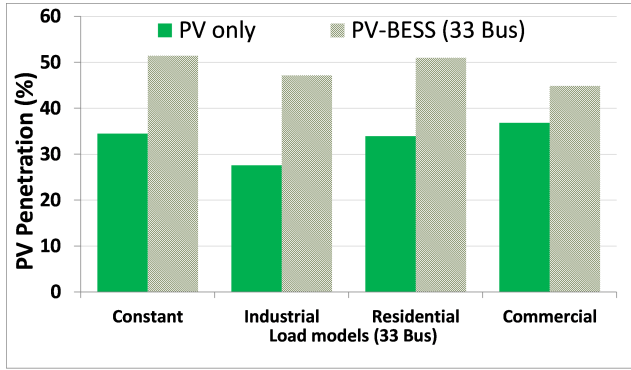


**FIGURE 15.** The comparison of PV penetration of B-SDPVG plant with PV only in IEEE 33 bus distribution network.

each time varying voltage dependent load model causes an additional reduction in total energy losses of about 18% in IEEE 33 bus and about 24 % in IEEE 69 bus distribution networks. The comparison of the reduction in energy losses with PV and PV-BESS in IEEE 33 and IEEE 69 bus networks is shown in FIGURE. 9 and FIGURE. 10. The hourly power losses for base case, with PV only and with B-SDPVG plant in IEEE 33 and IEEE 69 bus distribution networks are plotted in FIGURE. 11 and FIGURE. 12.

### C. IMPACT ON BUS VOLTAGE PROFILE

In comparison to the PV only, the addition of BESS units resulted in bringing more enhancements to bus voltage profiles in both distribution networks. The voltage magnitudes of weakest bus in the base case, with PV only and with B-SDPVG plant in each time varying voltage dependent load model for both distribution networks are plotted in FIGURE. 13 and FIGURE. 14.

### D. IMPACT ON PENETRATION LEVELS

Furthermore, B-SDPVG plant was found favorable than the case of PV only in terms on penetration levels. The size of the PV plants in both distribution networks was increased due to the addition of BESS units. Due to the increment in the sizes of PV plants, the total energy produced in B-SDPVG plant was higher than the total energy produced in PV only, which ultimately helped to increase the plant penetration levels of B-SDPVG plant. The penetration levels of each time varying voltage dependent load model in IEEE 33 bus and IEEE 69 bus distribution network are shown in FIGURE. 15 and FIGURE. 16.

With PV alone, the penetration levels in IEEE 33 bus distribution network for different time varying load dependent load models was ranging in between 15 % to 29 %. Whereas, with B-SDPVG, the penetration levels for the same network was ranging in between 33 % to 40 %. Additionally, with PV only in IEEE 69 bus distribution network, the penetration levels for different time varying load dependent load models was ranging in 20 % to 38 %. Whereas, with B-SDPVG, the penetration levels for the same network was ranging in 42 % to 54 %.

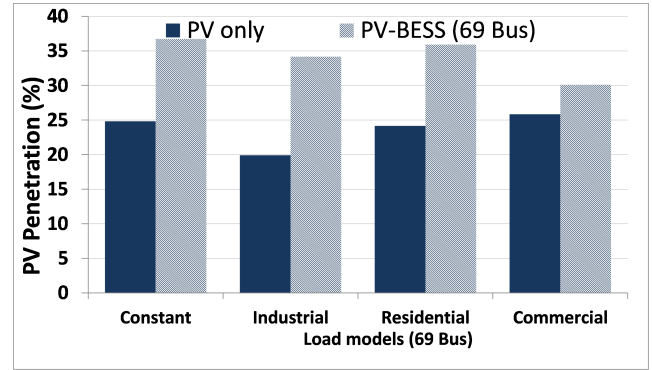


**FIGURE 16.** The comparison of PV penetration of B-SDPVG plant with PV only in IEEE 69 bus distribution network.

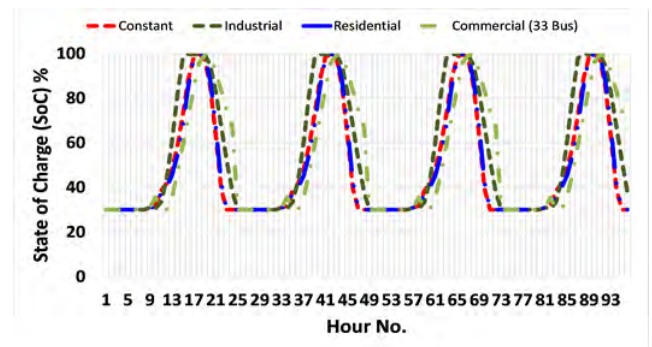


**FIGURE 17.** The battery state-of-charge (SoC) in IEEE 33 bus network.

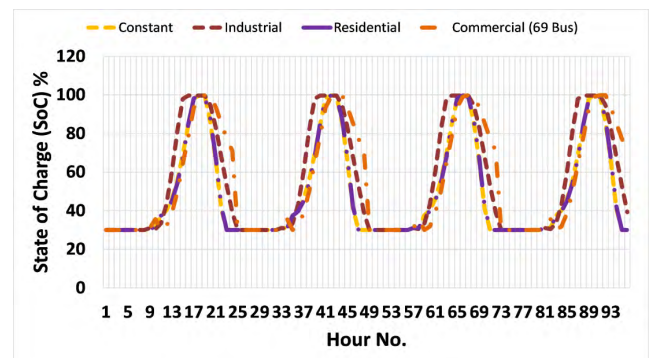


**FIGURE 18.** The battery state-of-charge (SoC) in IEEE 69 bus network.

The sizes of PV plants and BESS unit, and their penetration levels for each load models in both distribution networks were observed to be varying from each other. Therefore, it could be established that electrical network design and types of load play an important role in determining the sizes of PV plants and battery storage.

### E. IMPACT ON STATE-OF-CHARGE (SOC)

In order to remain in safe state, the SoC of the batteries during every hour was kept according to the defined constrained. From the results, it was seen, SoC during the operation remained in between 30 % and 100 %. The SoC

increased during the sunny hours due to charging from the PV power and decreased at night due to discharging. The SoC of the battery storage during every hour is displayed in FIGURE. 17 and FIGURE. 18.

## VI. CONCLUSION

The paper presents a Mixed Integer Optimization using Genetic Algorithm (MIOGA) for determining the optimum sizes and placements of Battery-Sourced Distributed Photovoltaic Generation (B-SDPVG) plants to reduce the total energy losses in distribution networks. In the proposed framework the sizes of the PV plant, the battery storage and the optimum levels of energy requirements were determined dynamically. Total energy losses Index (TELI) was formulated as the main objective function for the optimization problem. The bus voltage deviations and penetrations of the Battery-Sourced Distributed Photovoltaic Generation (B-SDPVG) plants were also calculated. In order to assess the stochastic behavior of solar irradiance, 15 years of weather data was modeled by using Beta Probability Density Function (Beta-PDF). The proposed algorithm was applied on IEEE 33 bus and IEEE 69 bus test distribution networks and optimum results were acquired for different time varying voltage dependent load models.

From the results obtained through this study, it was revealed that, the integration of Battery-Sourced Distributed Photovoltaic Generation (B-SDPVG) plants in the distribution networks resulted in higher penetration levels as compared to PV system acting alone. The introduction of BESS units in each time varying voltage dependent load model caused an additional reduction in total energy losses by about 18 % in IEEE 33 bus and 24 % in IEEE 69 bus distribution networks. With PV system without battery storage, the penetration levels in IEEE 33 bus distribution network for different time varying load dependent load models were ranging in 15 % to 29 %. Whereas, with B-SDPVG, the penetration levels for the same network were ranging in 33 % to 40 %. Also, in PV system without battery storage in IEEE 69 bus distribution network, the penetration levels for different time varying load dependent load models were ranging in 20 % to 38 %. Whereas, with B-SDPVG, the penetration levels for the same network were ranging in 42 % to 54 %.

As compared to bus voltage profiles in base case and in PV alone, the improvements in the voltage deviation due to addition of battery storage was significant. The proposed algorithm was found effective in reducing the amount of energy losses, enhancing voltage profiles and increasing penetrations of the PV plants.

The scope of this study was limited to the sizing and utilization of energy from B-SDPVG. Only technical benefits of batteries at distribution level were considered. However, addition of batteries increases the cost of the PV system. Therefore, it is recommended that future studies related to PV system with batteries should consider the impact of batteries on the cost of the PV systems.

## ACKNOWLEDGMENTS

The authors would like to thank Universiti Teknologi PETRONAS (UTP) for providing the graduate assistantship (GA) for this work.

## REFERENCES

- [1] N. Boutana, A. Mellit, V. Lughi, and A. M. Pavan, "Assessment of implicit and explicit models for different photovoltaic modules technologies," *Energy*, vol. 122, pp. 128–143, Mar. 2017.
- [2] M. Aman *et al.*, "A review of safety, health and environmental (SHE) issues of solar energy system," *Renew. Sustain. Energy Rev.*, vol. 41, pp. 1190–1204, Jan. 2015.
- [3] V. Devabhaktuni, M. Alam, S. S. S. R. Depuru, R. C. Green, D. Nims, and C. Near, "Solar energy: Trends and enabling technologies," *Renew. Sustain. Energy Rev.*, vol. 19, pp. 555–564, Mar. 2013.
- [4] IPVPS. (2015). *Snapshot of Global Photovoltaic Markets*. Accessed: May 4, 2017. [Online]. Available: [http://www.iea-pvps.org/index.php?id=3&eID=dam\\_frontend\\_push&docID=3584](http://www.iea-pvps.org/index.php?id=3&eID=dam_frontend_push&docID=3584)
- [5] SolarPower Europe, "Global market outlook for solar power 2015–2019," European Photovoltaic Industry Association, Brussels, Belgium, Tech. Rep. 9789082228410, 2015.
- [6] S. Teleke, M. E. Baran, S. Bhattacharya, and A. Q. Huang, "Rule-based control of battery energy storage for dispatching intermittent renewable sources," *IEEE Trans. Sustain. Energy*, vol. 1, no. 3, pp. 117–124, Oct. 2010.
- [7] M. Z. Daud, A. Mohamed, and M. A. Hannan, "An improved control method of battery energy storage system for hourly dispatch of photovoltaic power sources," *Energy Convers. Manage.*, vol. 73, pp. 256–270, Sep. 2013.
- [8] B. Bhargava and G. Dishaw, "Application of an energy source power system stabilizer on the 10 MW battery energy storage system at Chino substation," *IEEE Trans. Power Syst.*, vol. 13, no. 1, pp. 145–151, Feb. 1998.
- [9] Z. Wang, J. Ma, and L. Zhang, "Finite element thermal model and simulation for a cylindrical Li-ion battery," *IEEE Access*, vol. 5, pp. 15372–15379, 2017.
- [10] A. A. Jamali, N. M. Nor, and T. Ibrahim, "Energy storage systems and their sizing techniques in power system—A review," in *Proc. IEEE Conf. Energy Convers. (CENCON)*, Oct. 2015, pp. 215–220.
- [11] X. Hu, Y. Zou, and Y. Yang, "Greener plug-in hybrid electric vehicles incorporating renewable energy and rapid system optimization," *Energy*, vol. 111, pp. 971–980, Sep. 2016.
- [12] Z. Wang, J. Hong, P. Liu, and L. Zhang, "Voltage fault diagnosis and prognosis of battery systems based on entropy and Z-score for electric vehicles," *Appl. Energy*, vol. 196, pp. 289–302, Jun. 2017.
- [13] X. Wu, X. Hu, S. Moura, X. Yin, and V. Pickert, "Stochastic control of smart home energy management with plug-in electric vehicle battery energy storage and photovoltaic array," *J. Power Sources*, vol. 333, pp. 203–212, Nov. 2016.
- [14] X. Hu, C. Zou, C. Zhang, and Y. Li, "Technological developments in batteries: A survey of principal roles, types, and management needs," *IEEE Power Energy Mag.*, vol. 15, no. 5, pp. 20–31, Sep./Oct. 2017.
- [15] L. Zhang, X. Hu, Z. Wang, F. Sun, and D. G. Dorrell, "A review of supercapacitor modeling, estimation, and applications: A control/management perspective," *Renew. Sustain. Energy Rev.*, vol. 81, pp. 1868–1878, Jan. 2017.
- [16] L. Zhang, X. Hu, Z. Wang, F. Sun, and D. G. Dorrell, "Fractional-order modeling and State-of-Charge estimation for ultracapacitors," *J. Power Sources*, vol. 314, pp. 28–34, May 2016.
- [17] A. González, E. Goikolea, J. A. Barrena, and R. Mysyk, "Review on supercapacitors: Technologies and materials," *Renew. Sustain. Energy Rev.*, vol. 58, pp. 1189–1206, May 2016.
- [18] A. A. Jamali, N. M. Nor, T. Ibrahim, and M. F. Romlie, "An analytical approach for the sizing and siting of battery-sourced inverters in distribution networks," in *Proc. 6th Int. Conf. Intell. Adv. Syst. (ICIAS)*, Aug. 2016, pp. 1–6.
- [19] N. Acharya, P. Mahat, and N. Mithulananthan, "An analytical approach for DG allocation in primary distribution network," *Int. J. Elect. Power Energy Syst.*, vol. 28, pp. 669–678, Dec. 2006.
- [20] D. Q. Hung, N. Mithulananthan, and R. C. Bansal, "Analytical strategies for renewable distributed generation integration considering energy loss minimization," *Appl. Energy*, vol. 105, pp. 75–85, May 2013.



- [21] D. Q. Hung and N. Mithulananthan, "Loss reduction and loadability enhancement with DG: A dual-index analytical approach," *Appl. Energy*, vol. 115, pp. 233–241, Feb. 2014.
- [22] W. L. Theo, J. S. Lim, W. S. Ho, H. Hashim, and C. T. Lee, "Review of distributed generation (DG) system planning and optimisation techniques: Comparison of numerical and mathematical modelling methods," *Renew. Sustain. Energy Rev.*, vol. 67, pp. 531–573, Jan. 2017.
- [23] M. Ahmadigorji and N. Amjadi, "Optimal dynamic expansion planning of distribution systems considering non-renewable distributed generation using a new heuristic double-stage optimization solution approach," *Appl. Energy*, vol. 156, pp. 655–665, Oct. 2015.
- [24] A. Zeinalzadeh, Y. Mohammadi, and M. H. Moradi, "Optimal multi objective placement and sizing of multiple DGs and shunt capacitor banks simultaneously considering load uncertainty via MOPSO approach," *Int. J. Elect. Power Energy Syst.*, vol. 67, pp. 336–349, May 2015.
- [25] M. H. Moradi and M. Abedini, "A combination of genetic algorithm and particle swarm optimization for optimal DG location and sizing in distribution systems," *Int. J. Elect. Power Energy Syst.*, vol. 34, pp. 66–74, Jan. 2012.
- [26] K. M. Muttaqi, A. D. T. Le, J. Aghaei, E. Mahboubi-Moghaddam, M. Negnevitsky, and G. Ledwich, "Optimizing distributed generation parameters through economic feasibility assessment," *Appl. Energy*, vol. 165, pp. 893–903, Mar. 2016.
- [27] D. F. Al Riza and S. I.-H. Gilani, "Standalone photovoltaic system sizing using peak sun hour method and evaluation by TRNSYS simulation," *Int. J. Renew. Energy Res.*, vol. 4, no. 1, pp. 109–114, 2014.
- [28] T. Ma, H. Yang, and L. Lu, "A feasibility study of a stand-alone hybrid solar-wind-battery system for a remote island," *Appl. Energy*, vol. 121, pp. 149–158, May 2014.
- [29] M. R. Singaravel and S. A. Daniel, "Studies on battery storage requirement of PV fed wind-driven induction generators," *Energy Convers. Manage.*, vol. 67, pp. 34–43, Mar. 2013.
- [30] H. Bhoje and G. Sharma, "An analysis of one MW photovoltaic solar power plant design," *Int. J. Adv. Res. Elect., Electron. Instrum. Eng.*, vol. 3, no. 1, pp. 6969–6973, 2014.
- [31] J. K. Kaldellis, D. Zafirakis, and E. Kondili, "Optimum sizing of photovoltaic-energy storage systems for autonomous small islands," *Int. J. Elect. Power Energy Syst.*, vol. 32, pp. 24–36, Jan. 2010.
- [32] C. Budischak, D. Sewell, H. Thomson, L. Mach, D. E. Veron, and W. Kempton, "Cost-minimized combinations of wind power, solar power and electrochemical storage, powering the grid up to 99.9% of the time," *J. Power Sources*, vol. 225, pp. 60–74, Mar. 2013.
- [33] W. Liu, S. Niu, and H. Xu, "Optimal planning of battery energy storage considering reliability benefit and operation strategy in active distribution system," *J. Mod. Power Syst. Clean Energy*, vol. 5, no. 2, pp. 177–186, 2017.
- [34] D. Q. Hung, N. Mithulananthan, and R. C. Bansal, "Integration of PV and BES units in commercial distribution systems considering energy loss and voltage stability," *Appl. Energy*, vol. 113, pp. 1162–1170, Jan. 2014.
- [35] W. Cao, J. Wu, N. Jenkins, C. Wang, and T. Green, "Benefits analysis of Soft Open Points for electrical distribution network operation," *Appl. Energy*, vol. 165, pp. 36–47, Mar. 2016.
- [36] C. Wang, G. Song, P. Li, H. Ji, J. Zhao, and J. Wu, "Optimal siting and sizing of soft open points in active electrical distribution networks," *Appl. Energy*, vol. 189, pp. 301–309, Mar. 2017.
- [37] J. Xiao, Z. Zhang, L. Bai, and H. Liang, "Determination of the optimal installation site and capacity of battery energy storage system in distribution network integrated with distributed generation," *IET Generat., Transmiss. Distrib.* vol. 10, no. 3, pp. 601–607, 2016. [Online]. Available: <http://digital-library.theiet.org/content/journals/10.1049/iet-gtd.2015.0130>
- [38] J. Sardi, N. Mithulananthan, M. Gallagher, and D. Q. Hung, "Multiple community energy storage planning in distribution networks using a cost-benefit analysis," *Appl. Energy*, vol. 190, pp. 453–463, Mar. 2017.
- [39] D. Q. Hung, Z. Y. Dong, and H. Trinh, "Determining the size of PHEV charging stations powered by commercial grid-integrated PV systems considering reactive power support," *Appl. Energy*, vol. 183, pp. 160–169, Dec. 2016.
- [40] N. Jayasekara, M. A. S. Masoum, and P. J. Wolfs, "Optimal operation of distributed energy storage systems to improve distribution network load and generation hosting capability," *IEEE Trans. Sustain. Energy*, vol. 7, no. 1, pp. 250–261, Jan. 2016.
- [41] A. Beiranvand, M. M. Aghdam, L. Li, S. Zhu, and J. Zheng, "Finding the optimal place and size of an energy storage system for the daily operation of microgrids considering both operation modes simultaneously," in *Proc. IEEE Int. Conf. Power Syst. Technol. (POWERCON)*, Sep/Oct. 2016, pp. 1–6.
- [42] M. R. B. Khan, R. Jidin, and J. Pasupuleti, "Multi-agent based distributed control architecture for microgrid energy management and optimization," *Energy Convers. Manage.*, vol. 112, pp. 288–307, Mar. 2016.
- [43] Z. Jinquan, Z. Zefeng, Y. Yiping, L. Changnian, and W. Wenhui, "Optimal charging/discharging scheme of battery storage systems in active distribution network," in *Proc. IEEE Power Energy Soc. Gen. Meeting (PESGM)*, Jul. 2016, pp. 1–5.
- [44] *MATLAB Version 8.5.0.197613 (R2015a)*. Natick, MA, USA: The MathWorks, Inc., 2015.
- [45] A. Sanfilippo, L. Martin-Pomares, N. Mohandes, D. Perez-Astudillo, and D. Bachour, "An adaptive multi-modeling approach to solar nowcasting," *Solar Energy*, vol. 125, pp. 77–85, Feb. 2016.
- [46] Y. M. Atwa, E. F. El-Saadany, M. M. A. Salama, and R. Seethapathy, "Optimal renewable resources mix for distribution system energy loss minimization," *IEEE Trans. Power Syst.*, vol. 25, no. 1, pp. 360–370, Feb. 2010.
- [47] M. Fan, V. Vittal, G. T. Heydt, and R. Ayyanar, "Probabilistic power flow studies for transmission systems with photovoltaic generation using cumulants," *IEEE Trans. Power Syst.*, vol. 27, no. 4, pp. 2251–2261, Nov. 2012.
- [48] D. Q. Hung, N. Mithulananthan, and K. Y. Lee, "Determining PV penetration for distribution systems with time-varying load models," *IEEE Trans. Power Syst.*, vol. 29, no. 6, pp. 3048–3057, Nov. 2014.
- [49] D. K. Khatod, V. Pant, and J. Sharma, "Evolutionary programming based optimal placement of renewable distributed generators," *IEEE Trans. Power Syst.*, vol. 28, no. 2, pp. 683–695, May 2013.
- [50] W.-S. Tan, M. Y. Hassan, M. S. Majid, and H. A. Rahman, "Optimal distributed renewable generation planning: A review of different approaches," *Renew. Sustain. Energy Rev.*, vol. 18, pp. 626–645, Feb. 2013.
- [51] A. E. Breiholz, K. M. Kronfeld, K. L. Walling, and R. J. McCabe, "Weather radar system and method with fusion of multiple weather information sources," Google Patents 9 535 158, Jan. 3, 2017.
- [52] NSRDB. (Mar. 15, 2016). *National Solar Radiation Data Base*. [Online]. Available: [http://rredc.nrel.gov/solar/old\\_data/nsrdb/](http://rredc.nrel.gov/solar/old_data/nsrdb/)
- [53] E. Bompard, E. Carpaneto, G. Chicco, and R. Napoli, "Convergence of the backward/forward sweep method for the load-flow analysis of radial distribution systems," *Int. J. Elect. Power Energy Syst.*, vol. 22, no. 7, pp. 521–530, 2000.
- [54] H. Shaker, H. Zareipour, and D. Wood, "Impacts of large-scale wind and solar power integration on California's net electrical load," *Renew. Sustain. Energy Rev.*, vol. 58, pp. 761–774, May 2016.
- [55] SMA. (Feb. 23, 2016). *Solar Technology AG Sunny Boy TL-US Series*. [Online]. Available: <http://files.sma.de/dl/10707/SUNNYBOY6-11TLUS-DUS144518W.PDF>
- [56] B. Chen, K. H. Kwan, and R. Tan, "Battery capacity planning for grid-connected solar photovoltaic systems," in *Proc. Asia-Pacific Signal Inf. Process. Assoc. Annu. Summit Conf. (APSIPA)*, Dec. 2014, pp. 1–5.
- [57] D. Q. Hung, N. Mithulananthan, and R. C. Bansal, "An optimal investment planning framework for multiple distributed generation units in industrial distribution systems," *Appl. Energy*, vol. 124, pp. 62–72, Jul. 2014.
- [58] P. F. Chairman, M. P. Bhavaraju, and B. E. Biggerstaff, "IEEE reliability test system: A report prepared by the reliability test system task force of the application of probability methods subcommittee," *IEEE Trans. Power App. Syst.*, vol. PAS-98, no. 6, pp. 2047–2054, Feb. 1979.
- [59] M. Jamil and A. S. Anees, "Optimal sizing and location of SPV (solar photovoltaic) based MLDG (multiple location distributed generator) in distribution system for loss reduction, voltage profile improvement with economical benefits," *Energy*, vol. 103, pp. 231–239, May 2016.
- [60] S. G. Naik, D. K. Khatod, and M. P. Sharma, "Sizing and siting of distributed generation in distribution networks for real power loss minimization using analytical approach," in *Proc. Int. Conf. Power, Energy Control (ICPEC)*, Feb. 2013, pp. 740–745.
- [61] R. W. Chang, N. Mithulananthan, and T. K. Saha, "Novel mixed-integer method to optimize distributed generation mix in primary distribution systems," in *Proc. 21st Austral. Univ. Power Eng. Conf. (AUPEC)*, Sep. 2011, pp. 1–6.

- [62] D. Q. Hung and N. Mithulananthan, "An optimal operating strategy of DG unit for power loss reduction in distribution systems," in *Proc. 7th IEEE Int. Conf. Ind. Inf. Syst. (ICIIS)*, Aug. 2012, pp. 1–6.
- [63] B. Venkatesh, R. Ranjan, and H. B. Gooi, "Optimal reconfiguration of radial distribution systems to maximize loadability," *IEEE Trans. Power Syst.*, vol. 19, no. 1, pp. 260–266, Feb. 2004.
- [64] J. O. G. Posada *et al.*, "Aqueous batteries as grid scale energy storage solutions," *Renew. Sustain. Energy Rev.*, vol. 68, pp. 1174–1182, Feb. 2017.
- [65] J. Johansen, "Fast-charging electric vehicles using AC," M.S. thesis, Tech. Univ. Denmark, Kongens Lyngby, Denmark, 2013.
- [66] C. Zou, C. Manzie, D. Nešić, and A. G. Kallapur, "Multi-time-scale observer design for state-of-charge and state-of-health of a lithium-ion battery," *J. Power Sources*, vol. 335, pp. 121–130, Dec. 2016.



**NURSYARIZAL MOHD NOR** received the Ph.D. degree in electrical power engineering from Universiti Teknologi PETRONAS (UTP), Malaysia, in 2009. He is currently a committed Associate Professor with over 16 years of research and academic experience with the Electrical and Electronics Engineering Department, UTP, where he has developed numerous projects on national and international level in frames of electrical protection box, portable thermoelectric generator, health monitoring system, and portable solar generator. He has authored numerous research articles in peer-reviewed international journals, book chapters, conferences, and symposiums. His research interests include specialization in power economics operation and control, power system analysis, and power system state estimation.



**ABID ALI** received the B.Sc. degree (Hons.) in electronics from the University of Sindh, Jamshoro, Pakistan, in 2007, and the M.Eng. degree in electrical power from Universiti Teknologi Malaysia, Johor Bahru, Malaysia, in 2012. He is currently pursuing the Ph.D. degree with the Electrical and Electronic Engineering Department, Universiti Teknologi PETRONAS, Perak, Malaysia. In 2012, he joined Osmani & Company, Pakistan, where he was involved in the development of 50-MW wind and 40-MW solar PV plants for the first smart city of Pakistan. His current research interests include the integration of battery storage for the utility-scale photovoltaic plants.



**TAIB IBRAHIM** was born in Kedah, Malaysia, in 1972. He received the B.Eng. degree (Hons.) in electrical and electronics engineering from Coventry University, U.K., in 1996, the M.Sc. degree in electrical power engineering from the University of Strathclyde, U.K., in 2000, and the Ph.D. degree in electrical machine design from The University of Sheffield, U.K., in 2009. He was with Airod (M) Sdn Bhd and Universiti Teknologi PETRONAS (UTP). He is currently the Cluster Leader of power, control, and instrumentation with UTP. His research interests range from electrical machines developments to their associated drives.



**MOHD FAKHIZAN ROMLIE** received the B.Eng. degree (Hons.) in electrical and electronic from Universiti Teknologi PETRONAS in 2004, the M.Eng. degree in power system engineering from The University of Western Australia in 2006, and the Ph.D. degree in electrical engineering from the University of Nottingham, U.K., in 2014. He is currently a Lecturer with Universiti Teknologi PETRONAS. His research interests include smart grid, renewable energy, and wireless power transfer.

• • •